ACS OMEGA

http://pubs.acs.org/journal/acsodf

Article

Highly Stretchable and Sensitive Single-Walled Carbon Nanotube-Based Sensor Decorated on a Polyether Ester Urethane Substrate by a Low Hydrothermal Process

Riyani Tri Yulianti, Yuyun Irmawati, Fredina Destyorini, Muhammad Ghozali, Andi Suhandi, Surip Kartolo, Andri Hardiansyah, Joon-Hyun Byun, Mohammad Hamzah Fauzi,* and Rike Yudianti*

Cite This: *ACS Omega* 2021, 6, 34866−34875

Read Online

ACCESS | Metrics & More | Article Recommendations

ABSTRACT: We report a highly stretchable sensor with low-concentration (1.5 wt %) single-walled carbon nanotubes (SWCNTs) on flexible polyether ester urethane (PEEU) yarn, fabricated using a low hydrothermal process at 90 °C. Although SWCNTs restrict the PEEU polymer chain mobility, the resulting ductility of our nanocomposites reduces only by 16.5% on average, initially from 667.3% elongation at break to 557.2%. The resulting electrical resistivity of our nanocomposites can be controlled systematically by the number of hydrothermal cycles. A high gauge factor value of 4.84 is achieved at a tensile strain below 100%, and it increases up to 28.5 with applying a tensile strain above 450%. We find that the piezoresistivity of our nanocomposite is sensitive to temperature variations of 25−85 °C due to the hopping effect, which promotes more charge transport at elevated temperatures. Our nanocomposites offer both a high sensitivity and a large strain sensing range, which is achieved with a relatively simple fabrication technique and low concentration of SWCNTs.

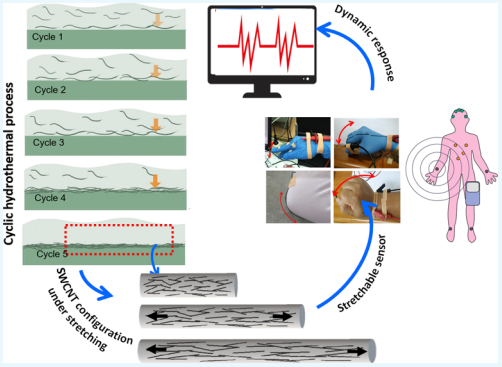

INTRODUCTION

Global demand and potential market for smart textile-based electronic and sensing devices are on the rise.[1] The surge is partly driven by the possibility to incorporate smart textiles into various aspects such as sensing elements in human motion detection systems,[2,3] personalized health monitoring systems,[4,5] human−machine interaction, and soft robotics.[2,6] A reliable wearable sensor should at least possess four basic characteristics, namely, high sensitivity, high stretchability, fast response, and good durability. These characteristics primarily are determined by its sensing element and substrate as well as their interfacial bonding. Carbon nanotubes (CNTs) are one of the active and promising elements for nanoreinforcements or fillers because of their extraordinary electromechanical properties and high specific surface areas. A highly sensitive surface of CNTs to the presence of mechanical perturbation makes CNTs a promising starting active element for super miniaturized electromechanical sensors and electrocatalytic material.[2,7] Both the properties of a highly sensitive surface and excellent electrical conductivity make CNTs an attractive building block for all wearable sensors. Although individual CNTs have all desirable properties, the performance hinges on and is determined by a network of CNTs on the substrate material. Therefore, materials for both the sensing element and substrate must be carefully selected and matched to meet the desired criteria. Various types of stretchable sensor platforms have been reported to date including hybrid graphene/ZnO/cotton,[8] CNT/thermoplastic polyurethane,[9] graphene/polydimethylsiloxane (PDMS),[10] Au/PDMS/PANI,[11] CNT/silicon rubber,[12] and ionic hydrogel,[13] which have different sensitivities in response. Various pathways and techniques to build smart textiles have been devised throughout the years ranging from wet spinning,[9,14,15] knife-rolled coating,[16] dip-coating,[17,18] and air spray coating.[19] However, further exploration in fabrication techniques is still required to find a simple process that is cost-effective and has large scale potential to produce wearable sensors with a good and reliable performance. Mixing CNTs directly with polymer substrates often suffers from a poor dispersion and requires high enough concentrations to achieve a certain desired resistance value. This results in high production costs and complicated engineering routes. The deposition of individual CNT solutions on the polymer surface is one of the more convenient techniques for fabricating CNT networks by surface mod-

Received: October 5, 2021
Accepted: November 23, 2021
Published: December 7, 2021

https://doi.org/10.1021/acsomega.1c05543
ACS Omega 2021, 6, 34866−34875

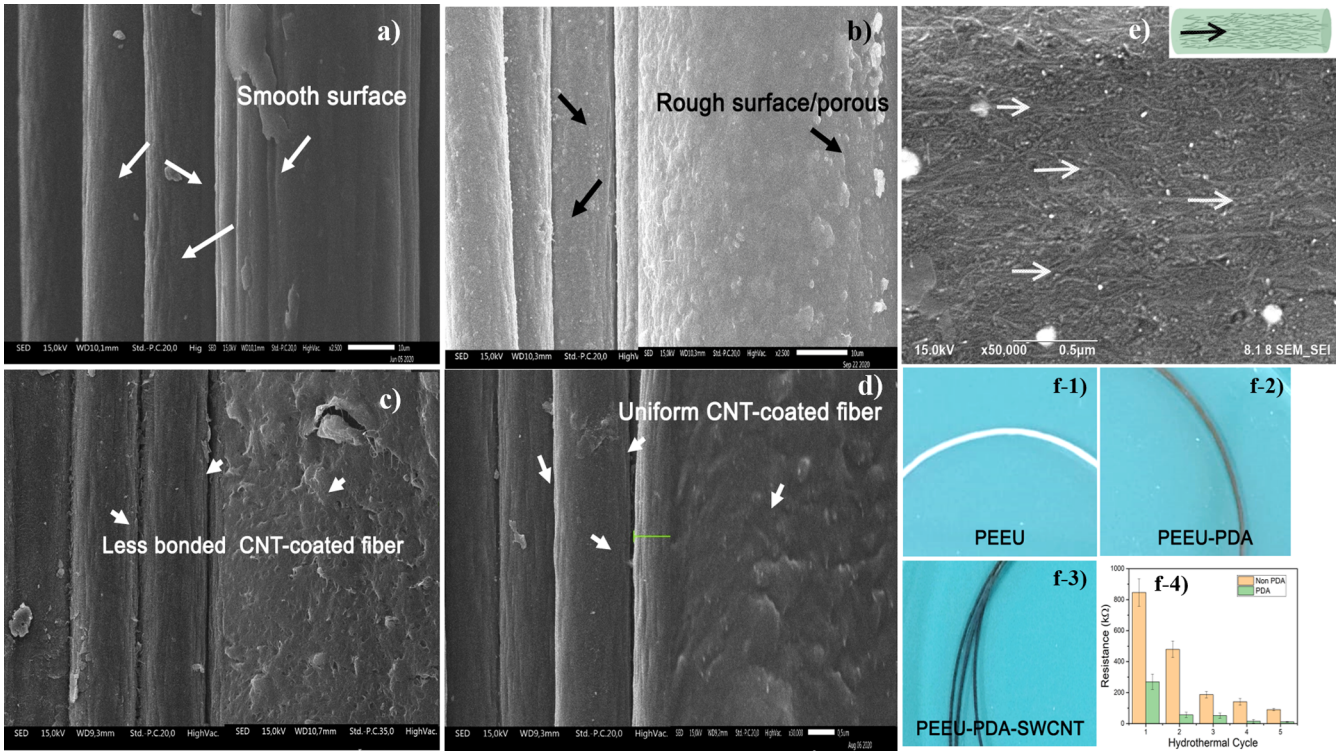

Figure 1. Morphological surface of the nanocomposite. (a) PEEU yarn. (b) PEEU yarn after PDA treatment. (c) Nanocomposite without PDA treatment. (d) Nanocomposite with PDA treatment. (e) Orientation of SWCNTs on the nanocomposite surface. (f-1) Bare PEEU yarn (white). (f-2) after polymerized-dopamine treatment (brown), (f-3) nanocomposite (black), and (f-4) hydrothermal cycle *vs* resistance of CNT−PEEU nanocomposite.

ification. Using the technique Li et al. successfully sprayed superhydrophobic coated CNT/TPE on a fabric glove,[19] Amjadi et al. successfully spray coated CNTs on Ecoflex with an excellent stretchability,[20] Dai et al. successfully deposited CNTs onto porous nonwoven fabric,[21] and Tang et al. successfully used CNT ink as the core solution to create a highly stretchable and durable core−sheath piezoresistive fiber.[15] The deposition technique is therefore crucial and promising to construct a good conductive network of CNTs on the matrix while maintaining all the desirable performance. However, the strategy to achieve simultaneously sensitive and highly flexible sensors using cost-effective fabrication techniques and materials remains a major challenge to date.

Here, we report the successful development of a facile route to fabricate single-walled CNT (SWCNT)-coated polyether ester urethane (PEEU) as a flexible, stretchable, and sensitive strain sensor by cyclic hydrothermal coating. We uniformly coated a thin polydopamine (PDA) layer onto PEEU yarn via *in situ* polymerization of dopamine to form SWCNT−substrate interfacial bonding. With this cyclic hydrothermal coating technique, we can convert an inexpensive commercially available PEEU yarn into a valuable piezoresistivity sensor with a controlled process and reusable nanosolution. This process has economical value and potential for large-scale production. With this fabrication technique, we can produce a piezoresistive sensor with both high sensitivity and good stretchability that can withstand extreme strains of up to 600%, a gauge factor (GF) of up to 28.5, and a fast response of less than 1 s with low CNT concentration. We evaluate and discuss all relevant electromechanical properties such as responsiveness and the sensitivity level of our nanocomposites in response to various mechanical deformation modes and controlled temperature variations.

RESULTS AND DISCUSSION

Structure and Physical Properties. The SWCNT network decorated on the PEEU yarn has an outstanding stretchability and response to the mechanical deformation. Figure 1 shows the structure and physical properties of the nanocomposites with and without PDA treatment as revealed by scanning electron microsopy images. Self-polymerization of dopamine on the PEEU yarn plays an essential role in strengthening SWCNT−PEEU interfacial bonding. The treatment altered the morphological surface of the PEEU yarn in such a way that it became more porous and had a hydrophilic surface, as shown in Figure 1b. Amine and hydroxyl-rich groups of PDA are responsible for altering the PEEU surface type from hydrophobic to hydrophilic. Having a hydrophilic contour means that the SWCNTs can be tightly embedded in the substrate (Figure 1d). In contrast, without PDA treatment, we observed a poor surface adhesion of the SWCNTs to the yarn as shown in Figure 1c. Then, we clearly observed a good adhesion between SWCNTs and the polymer substrate whereas SWCNTs tend to align along the PEEU substrate deeply. The degree of SWCNT orientation along the bulk substrate determines electron transport of the sensing properties of the nanocomposite, which is parallel to the tensile axis.[22]

Previous reports show that the primary amine group in PDA is indeed biocompatible and can be effectively used as a surface adherent coating for biomolecular systems.[23,24] Surface modification after PDA treatment is visibly seen with the naked eye where its color changed from white to brown,

https://doi.org/10.1021/acsomega.1c05543
ACS Omega 2021, 6, 34866−34875

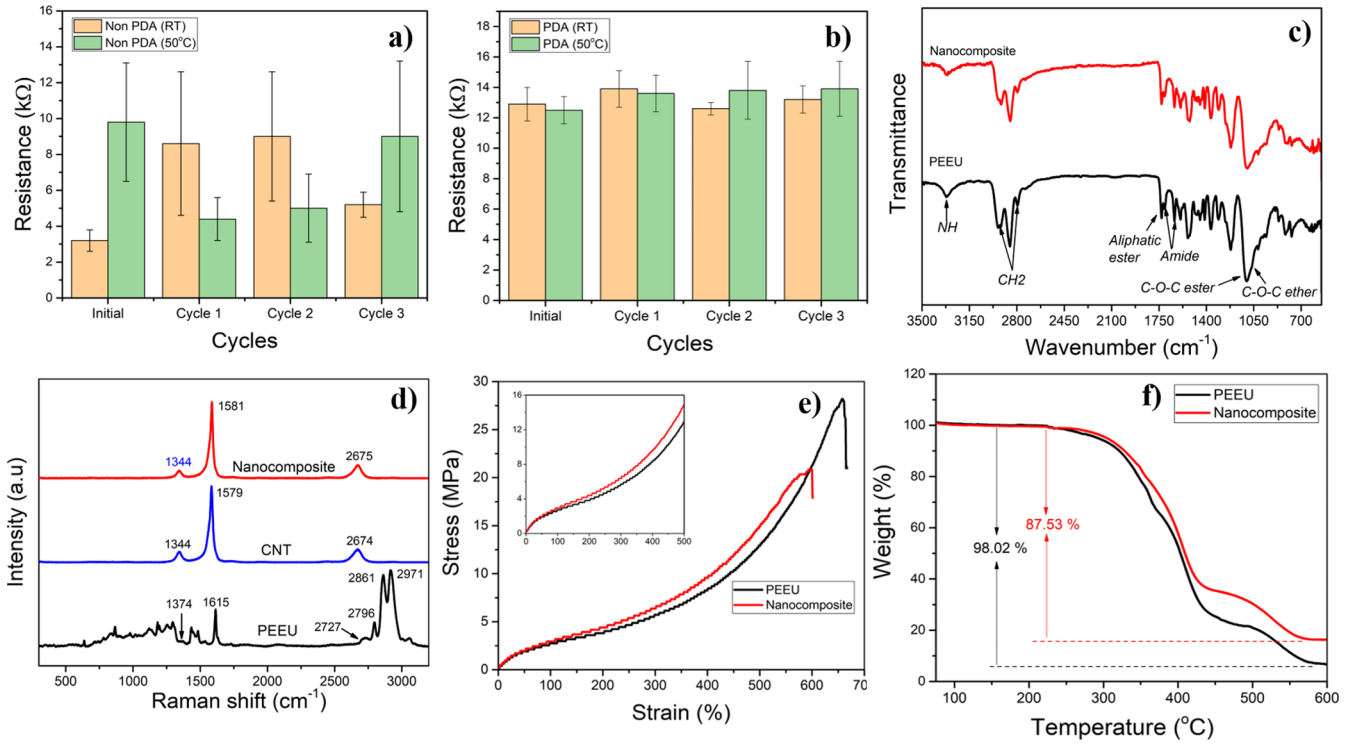

Figure 2. Wash durability of the nanocomposite. (a) Without and (b) with PDA treatment. (c) FTIR spectra. (d) Raman spectroscopy. (e) Stress−strain representative curve. (f) Thermal properties of bare PEEU yarn and SWCNT−PEEU nanocomposites.

indicating successful templating of polymerized PDA on the polymer substrate, as shown in Figure 1(f-2). We compare the surface absorption of bare PEEU yarn and PDA-polymerized PEEU yarn to the dispersed solution and record resistance change *versus* cycle number (Figure 1(f-4)). As a result, the PDA-polymerized surface rapidly absorbs SWCNTs and forms a network of tube elements as an electron transport pathway. The good stability of SWCNTs on the yarn surface not only guarantees a durable retention of molecules bound to its surface but also is the key factor to ensure long-term safe performance application. The hydrophilic surface has several active groups to facilitate faster absorption of SWCNTs that are responsible for the bonding stability and application performance.

A major challenge facing textile-based sensors is its durability in particular after being exposed to a harsh condition.[25] To examine the durability and reliability of our nanocomposites, we immersed them in water at room temperature and 50 °C and stirred at 100 rpm for 2 h. We repeat the cycle for three times and measure their electrical resistance after each cycle. For the nanocomposites with PDA treatment, the resistance value is almost unchanged throughout the cycles both at room temperature and 50 °C (Figure 2b). Furthermore, no visible discoloration is observed in water due to carbon or PDA. In contrast, for the nanocomposites without PDA treatment, we observe a very large resistance fluctuation throughout the cycles (48−181.45%), indicative of a weak interfacial bonding between SWCNTs and the yarn (Figure 2a). Intertube connection and the degree of nanotube alignment in bulk materials are crucial points to gain extraordinary electron transport and hence sensing properties. To this end, we conclude that PDA can protect the SWCNTs from being detached as well as retain the SWCNT configuration.

We have measured Fourier transform infrared (FTIR) and Raman spectra to gain insights of any functional groups present in the nanocomposites. As shown in Figure 2c, functional groups belonging to PEEU such as amine, alkyl, aliphatic ester, amide, COC ester, and COC ether groups can be easily identified from the FTIR spectra. The polymer is a three-block copolymer having satisfactory mechanical properties, degradability, nontoxicity, and excellent shape recovery properties.[26] The spectra obtained from bare PEEU yarn and nanocomposites are substantially similar in that we do not see a trace of SWCNTs in the spectra because they absorbed infrared light as expected. To observe SWCNT traces, we turn our attention to Raman spectroscopy. We were able to identify three successive Raman peaks, namely, D-band, G-band, and G′ band, from our nanocomposites, respectively. A defect-induced Raman peak in the graphitic structure (D-band) appeared around 1,344 cm^{-1}. An in-plane vibrational mode of sp^2 carbon atoms (G-band) appeared around 1,581 cm^{-1}. Finally, the G′ band, a second-harmonic Raman scattering of the D-band phonon, appeared around 2,675 cm^{-1}. The G-band spectrum shifts initially from 1,579 to a higher wavenumber, 1,581 cm^{-1}, indicating the presence of chemical interfacial interaction between SWCNTs and PEEU yarn whereas stress and charge transfer might occur. The shifting of the G-band generally occurs in some CNT−polymeric nanocomposites, indicating each interaction between the components.[27,28] Raman spectroscopy of the polymer yarn shows the asymmetric stretch of CH_2 at 2,971 cm^{-1}, the symmetric stretch of CH_3 at 2,861 cm^{-1}, and CH_2CH_3 deformation at 1,448 cm^{-1}. The band located at 1,615 cm^{-1} comes from the double C═C bond of the heterocycle of urethane. These bands are not visible in the nanocomposite due to high Raman sensitivity for the carbon structure.[29]

https://doi.org/10.1021/acsomega.1c05543
ACS Omega 2021, 6, 34866−34875

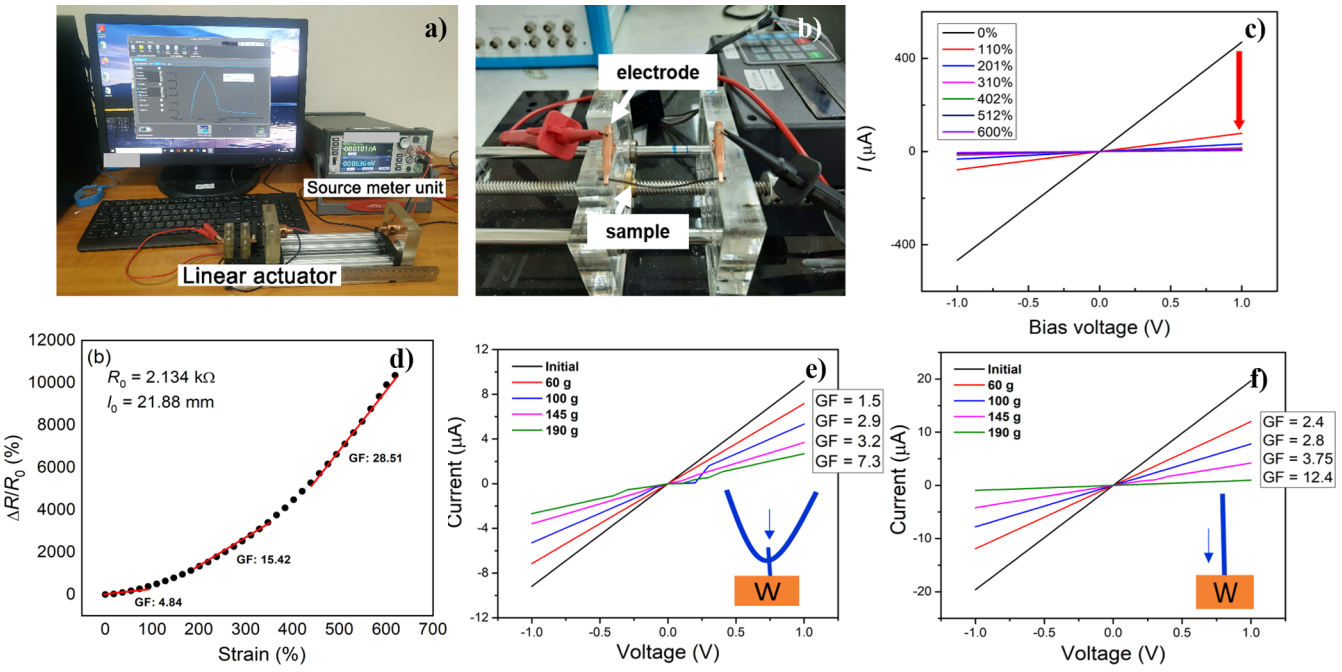

Figure 3. (a) Photograph of experimental set instruments. (b) Photograph of the linear actuator stage. (c) Selected IV curve recorded before (black curve) and after stretched to a various degree. (d) Normalized change in resistance plotted as a function of strain extracted from the IV curve displayed in panel (b). Current−voltage curve of the nanocomposite yarn in transverse (e) and axial (f) forces by weight loading (60, 100, 145, and 190 g).

We have selected PEEU yarn as a substrate for several reasons primarily due to its strength and excellent stretchability, a suitable platform for wearable sensors. Mechanical properties of the bare yarn and the nanocomposite yarn are compared to know the effect of SWCNTs on strength and stretchable properties of the nanocomposite. As we can see from Figure 2e, the bare yarn is able to sustain a very large strain range of up to 600% at 28.2 MPa. Interestingly, even after hydrothermal processing of SWCNTs, its ductility does not reduce significantly and is able to sustain the strain up to 600%. SWCNTs restrict stretchability to be stiffer due to SWCNT reinforcement. Figure 2f shows SWCNT-altered thermal decomposition properties of the nanocomposite. SWCNTs increased the thermal decomposition of the nanocomposite from 325 °C to about 340 °C which resulted in residues of 4.98 and 10.47% for bare yarn and the nanocomposite, respectively. The resulting residue is likely derived from PDA and nanotube substituents due to the thermal stability of CNTs.[30,31] The enhancement of the thermal stability of the nanocomposite is also affected by the yarn interface effect and the SWCNT interaction. A concentration of 1.5% nanotubes on the substrate also effectively increased Young's modulus by 14.3% where Young's modulus for the substrate and nanocomposites is 3.58 and 4.22 GPa, respectively. The values for optimizing the reinforcing effect of SWCNTs in polymer substrates include the quality of the SWCNT dispersion and the interfacial adhesion between the SWCNTs and the polymer substrate. This shows that SWCNTs are promising for the fabrication of polymer nanocomposites that possess strong potential for a wide spectrum of applications.

Electromechanical Responses. After exhaustively evaluating all relevant physical and structural properties of our nanocomposites, we are now in position to finally test their electromechanical responses. The sensor detection and responsiveness were real-time recorded due to an external interference effect such as mechanical strain. We placed the sample in a customized linear actuator where both sample ends were clamped firmly to copper electrodes as shown in Figure 3a,b. The sample under test had an initial length l_0 of 21.88 mm and resistance R_0 of 2.134 kΩ. We have measured a handful of samples from different batches and obtained consistently similar performance. Figure 3c shows selected VI curves for several strain values, from 0 to 600%. As one can see, the slope sharply reduced when we stretched the sample to 110% from its initial length, after which the slope gradually reduced. Note that the current only flows through the SWCNT network and the PEEU itself is an insulator and therefore does not conduct current. The transport across the sample relies heavily on the cross-linked network contact between each SWCNT constituent. When the sample is stretched, the cross-link effectively reduces, and consequently, the sample becomes less and less conducting. To evaluate the sensitivity of our nanocomposites to the applied strain, we plot a percentage change in the resistance with respect to its initial value ($\Delta R/R_0$) as a function of strain. The sensitivity is customarily denoted by a GF and the slope of $\Delta R/R_0$ *versus* strain. The GF value extracted from Figure 3d is not constant but strain-dependent, similar to previous reports.[9,32] Below 100% strain, we obtain a reasonably good sensitivity with a GF value of about 4.84. The sensitivity improves at a higher strain regime, reaching a GF value of about 28.5 above 450% strain. Although the GF value at low strain is relatively low, about 4.8, because the initial resistance typically is quite high, about 2 kΩ, and the resistance change (ΔR = GF × R_0 × ε) is still reasonably high and can be detected without using a special technique like a resistance bridge. For instance, for ε = 10% and GF = 4.8, we have a ΔR of about 1 kΩ.

We applied a mechanical stress to the nanocomposite yarn in transverse and axial directions. Mechanical stress such as

https://doi.org/10.1021/acsomega.1c05543
ACS Omega 2021, 6, 34866−34875

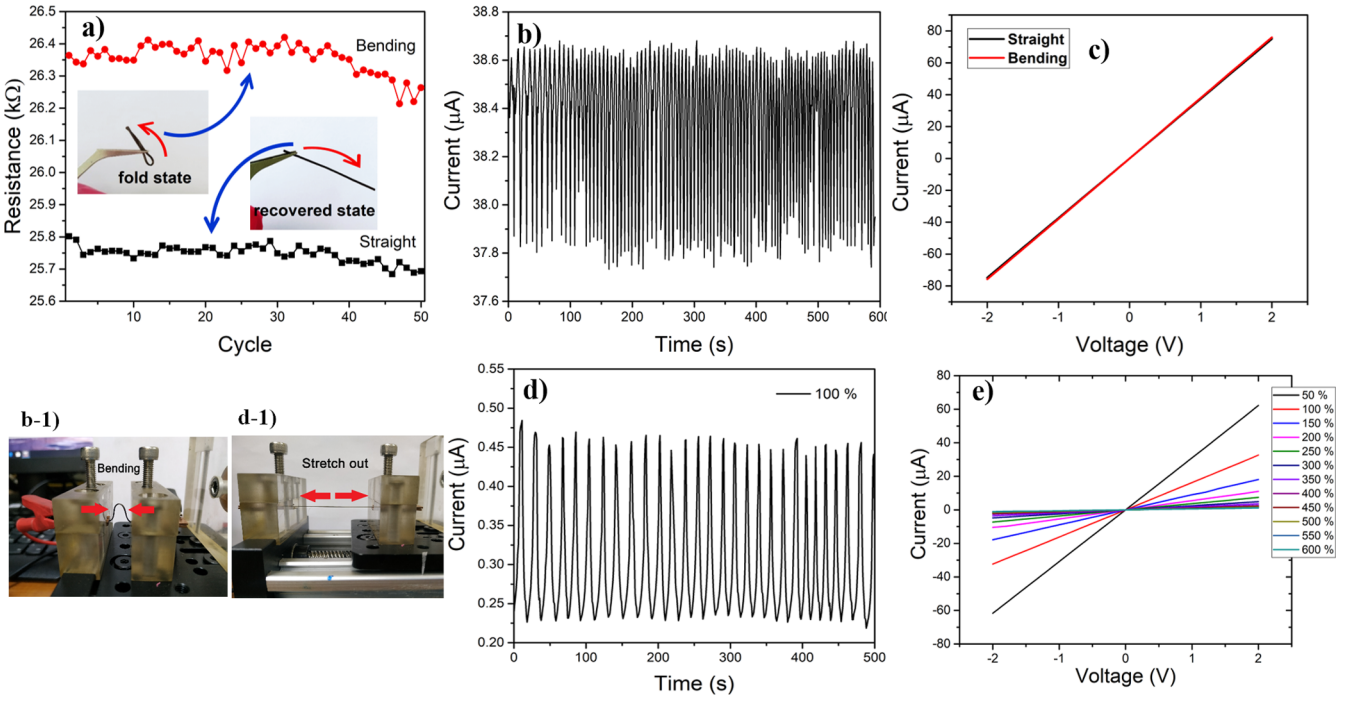

Figure 4. (a) Resistance changes in the fold−release cycle. (b) Current−time curve of bending−release cycles. (c) I−V curve of the bending−release cycles. (d) Current−time curve of stretch−release cycles. (e) Sweep of the stretch−release cycle. Photograph of the bending state (b-1) and stretching state (d-1) in the linear motor stage.

axial and transverse forces using weight loads of 60, 100, 145, and 190 g was subjected to our sample. We then compared these force directions on the nanocomposite sensitivity. Transversely, we put weight loads in the center of the nanocomposite yarn and the resulting voltage−current curves are shown in Figure 3e. Transverse weight loads of 60 to 190 g stretch the nanocomposite fiber from 25.9 up to 67.0%, corresponding to an increase in GF from 1.5 to 7.3. We also clamped the same weight load of 60 to 190 g at one end of the nanocomposite yarn in the axial direction. The axial weight loads stretch the nanocomposite fiber more than the previous case from 33.3 up to 282.0%, respectively (Figure 3f). In both force directions, the nanocomposites exhibit simultaneously electric current drops and a gradual increase in the GF with increasing weight load. For instance, the axial mechanical stress greatly reduces the electric current which corresponds well to the generation of nanocomposites that are more sensitive with GF value increases from 2.4 to 12.4. These observations suggest that the weight is not the only factor that must be considered but the force direction is also important in determining the sensitivity of the sensor.

We further test the nanocomposite under a mechanical cycle at several levels of applied strain to monitor its sensitivity and durability. PEEUs as a polymer substrate featured an ability to recover the original shape from the deformation state. The mechanical treatment, that is, fold-release cycle, was applied to the nanocomposites to investigate the shape recovery effect on the sensing properties. The nanocomposite retains its shape after folding as indicated by the simultaneous return in electrical resistance to the initial state (Figure 4a). In the first few fold−release cycles, the resistance was increased by ∼0.55−1.0% and was highly reproducible afterwards, no significant fluctuation was clearly observed. This could be due to the permanent replacement of some SWCNTs within the PEEU substrate in the first cycle. We put the sample in the customized linear actuator stage where two ends of the sample were tightly clamped. Both sample ends were clamped in 1.66 cm distance to control the movement in the actuator stage. The sensing response was real-time recorded under different mechanical mode cycles, that is, bending−straight and stretch−straight cycles. In bending−straight treatment over 900 cycles, the sample was bent to 79.5% and straightened to the initial length. The sample exhibits a sufficiently stable and durable response for 600 s, shown in Figure 4b, and did not show a significant resistive deformation after several cycles compared to the initial state (Figure 4c). Then, we treated the nanocomposite yarn in a larger-scale force by pulling it from 25 up to 600% elongation by the linear actuator stage. The stretch−straight cycle for 500 s was applied to the sample and real-time recorded. Figure 4d shows a 100% stretch−release cycle showing a stable and durable response under each cycle for 500 s. A large range of elongation of up to 600% causes a mechanical deformation of the electrical network in the nanocomposite structure. This is clearly indicated in the gradual decrease in electrical current of the nanocomposite yarn (Figure 4e).

In the various cycle scenarios, that is, fold−release, bending−straight, and stretch−straight cycles, our nanocomposite consistently show good linearity, sensitivity, and durability. We observe a change in the baseline resistance of the nanocomposite for each stretch treatment which may be due to the stress relaxation nature of the PEEU yarn.[12,33] External tension applied to the nanocomposites induces a stress transfer from the PEEU yarn to the SWCNT−PEEU nanocomposites and rearrangement and reorientation of SWCNTs. Tensile stress is slightly reduced by the stress relaxation effect and reconnection tube element. Therefore, the initial electrical resistance tends to be higher and then gradually decreases after the 120−200 s cycle period.

https://doi.org/10.1021/acsomega.1c05543
ACS Omega 2021, 6, 34866−34875

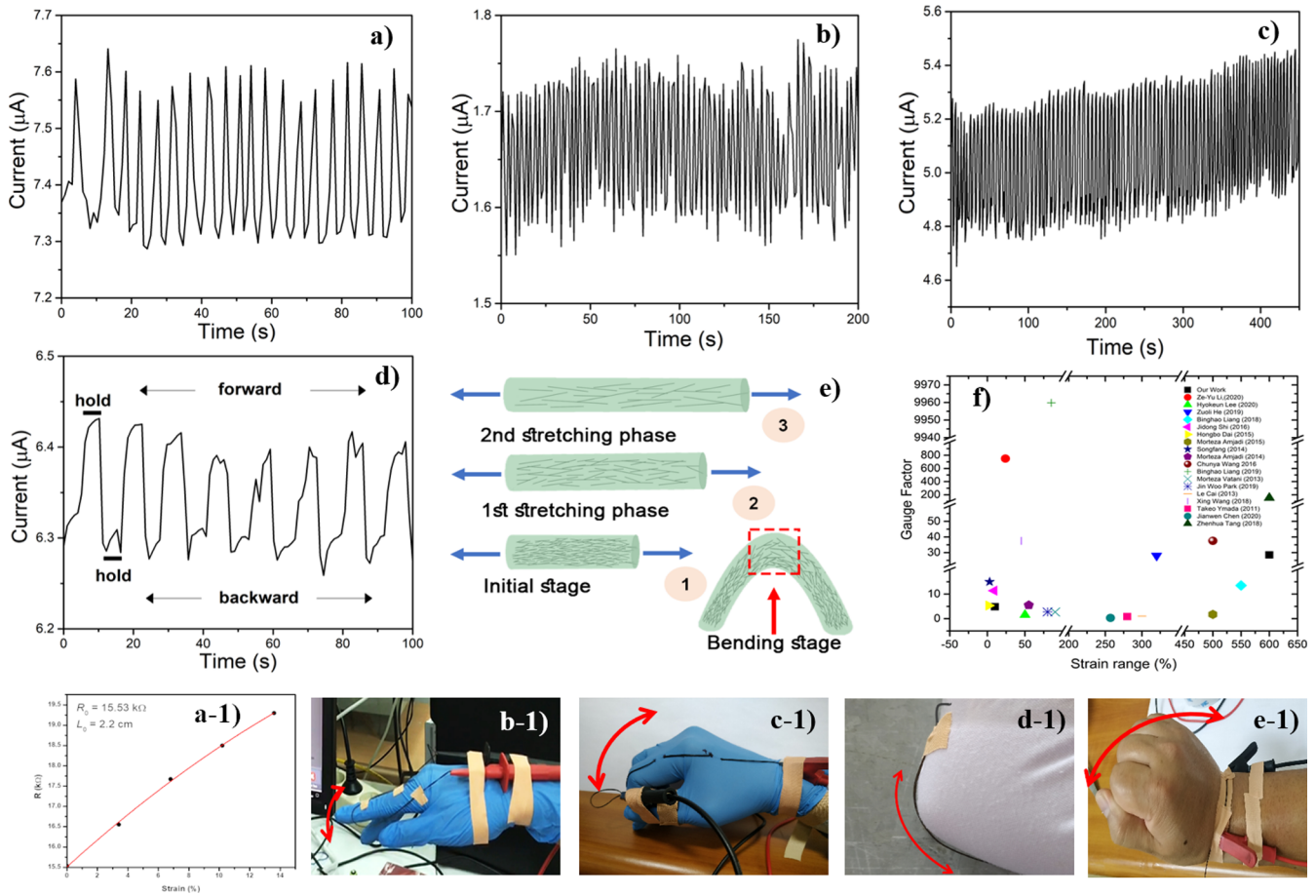

Figure 5. Dynamic response of the PEEU−SWCNT wearable sensor. (a) Sensing curve of the finger motion test. (b) Sensing curve of the open−clasping hand motion test. (c) Sensing curve of elbow flexion; (d) sensing curve of wrist motion. (e) Schematic model of the SWCNT configuration. (f) Comparison of the GF and max. strain between our strain sensor and the reported strain sensor. (a-1) Resistance response in low finger flexion. Photographs of the (b-1) index finger, (c-1) open−clasping hand motion, (d-1) elbow flexion, and (e-1) wrist motion.

Our nanocomposites responded well not only to the static strain but also to the dynamical strain. We have assembled our nanocomposites into a wearable sensor to detect dynamic motion as shown in Figure 5(b-1)−(e-1). An adhesive tape was used to fix both ends of the sensor for a stable connection. We attached a string of our nanocomposites to an index finger and see how it responded to a 90° flexing movement of the index finger. The electric current dropped when it flexed and vice versa with a characteristic response time of about 1 s. The wearable sensor shows a sensitive response of less than 1 s in a finger motion cycle with strain up to 10% (Figure 5a). We further recorded a dynamical strain of the nanocomposite in different motions. The nanocomposite yarn was fixed on the back hand to detect a sensing open−clasping hand motion (Figure 5b). The sensor shows an excellent sensitivity as well as responsivity with a response time of less than 1 s. The motion of the clasping hand imposes a strain onto the nanocomposite, which in turn reduced the electric current along the nanocomposites almost instantaneously. The electric current recovered back to its initial value when the action is reverted.

To evaluate our sensor for a large-scale movement, we fixed a 5 cm-long nanocomposite on the elbow joint. When the elbow was flexed to 145°, the nanocomposite fiber was stretched by about 20%. We repeated the movement over 50 cycles and recorded the corresponding electrical response simultaneously as shown in Figure 5c. As one can see, the response was stable over a long period of 400 s. We also assembled the fiber around the wrist to test the sensing capability for a cyclic transverse movement as shown in Figure 5d. The wrist was moved back and forth, but in between the movement, we rested for 5 s at each position. It is also crucial to know the threshold of our developed nanocomposite sensor for detecting human motion such as a small finger movement. We find that our nanocomposite attached to a finger still gives a noticeable electrical response when it gets a 4% stretch as shown in Figure 5a-1. It suggests that our nanocomposites could sense a fine human motion.

For all the dynamical strain scenarios presented above, our nanocomposites can detect various degrees of motion. This excellent electrical performance was achieved due to a strong interfacial bond between SWCNTs and the PEEU yarn. Furthermore, SWCNTs have excellent elastic properties,[34] enabling the CNTs to flexibly move as the PEEU yarn is stretched. From the whole electromechanical data presented above, we conclude that the mechanical deformation causes a change in the electrical conductivity of the nanocomposite yarn. The change in the electrical conductivity is due to the alteration in the network and configuration of the SWCNT element (Figure 5e). Prior to mechanical deformation, we consider that the initial configuration of tube elements aligned along the polymer chain which has the highest electrical

https://doi.org/10.1021/acsomega.1c05543
ACS Omega 2021, 6, 34866−34875

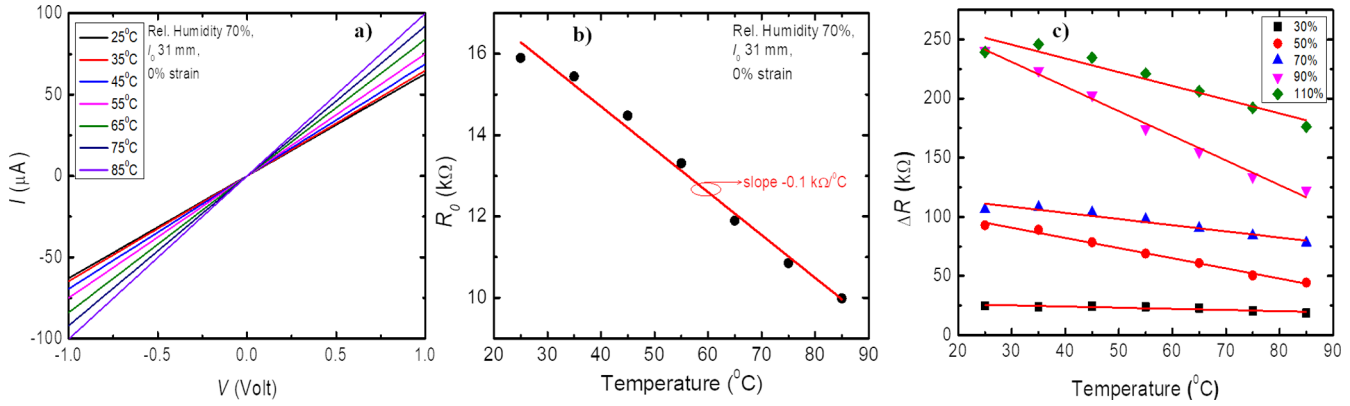

Figure 6. (a) VI curve of unstretched nanocomposites measured against chamber temperature variations ranging from 25 to 85 °C. The relative humidity of the chamber is fixed to 70%. (b) Initial resistance R_0 plotted as a function of temperature extracted from the VI curve in panel (a). (c) ΔR plotted as a function of temperature stretched ranging from 30 to 110%. The red lines in panels (b,c) are a linear fit to the data.

conductivity level. This analysis is in accordance with the morphological surface shown in Figure 1e and the initial stage of the exponential curve shown in Figure 3d. The alignment of the SWCNTs and the interconnection between them are an essential factor. The axial stretching applied to the nanocomposite causes a shearing force tube interconnection, giving rise to a direct reduction in the electrical conductivity of the nanocomposite yarn. Relaxing the nanocomposite yarn would make the CNTs reconnect and electron transport return to the initial state. Bending the nanocomposite might induce arc-shaped cracks and limit the conducting pathways. The SWCNT network and configuration in the PEEU polymer substrate are schematically illustrated in Figure 5e. The network and configuration dictate the electron transport properties because van der Waals and electrostatic interactions between CNTs are too weak to transfer electrons efficiently.[35,36]

Accordingly, SWCNT and PEEU interaction plays a vital role in the sensing and stretchability properties of the nanocomposite system. Some polymer substrates such as polyvinyl alcohol,[8,34,35] thermoplastic polyurethane,[36] polyvinyl carbonate,[37] PDMS,[38] and polyethylene terephthalate[39] were widely used as sensing element substrates which results in different stretchabilities and sensitivities of the sensor. The piezoresistive effect due to mechanical deformation of CNT/polymer composites can be understood in terms of the CNT network configuration, as investigated by many authors.[40−42]

We compare our nanocomposite sensor performance with some reported results, shown in Figure 5f. The figure shows the maximum working strain *versus* GF with different material substrates such as TPU/PDMS,[37] PMMA/PDMS,[10] PDMS/silicon oligomers,[38] PDMS,[38−44] ecoflex,[15,45] silk fabric/ecoflex,[46] epoxy resin,[47] and TPU[48,49] with different active elements such as graphene, CNTs, nanosilver, and carbon fabricated by various techniques. Some of these strain sensors possess GFs of up to a thousand with strains lower than 100%. Others can withstand a large strain over 200% with a GF lower than 20. Our nanocomposite presents a high stretchability of over 600% with a GF of 28.5, above the average value of the results reported which expectedly have a wide sensing range for many applications.

The linearity, stretchability, and durability of the PEEU−SWCNT nanocomposite-based strain sensors are mostly affected by the structure of the nanocomposite, the properties of the polymer substrate, and the interaction between the active element and the polymer matrix.[12,44,50] Furthermore, durability and sensitivity are mainly caused by the friction force between the filler elements and the matrix due to the slippage of fillers under stretching and the delay time associated with the re-establishment of the percolation network upon release.[51,52]

Investigating the piezoresistivity of our nanocomposites at a controlled temperature is needed to determine the thermal stability of their sensing performance. The piezoresistivity of CNT nanocomposites is known to be sensitive to temperature variations[53−55] To evaluate the effect, we put our nanocomposites inside a controlled temperature−humidity chamber and measure their transport properties. We investigate the piezoresistive properties against the temperature variations from 25 to 85 °C, while the relative humidity is fixed at 70% throughout the measurement. Figure 6a shows the VI curve of unstretched nanocomposites measured against the chamber temperature variations. The VI slope gradually gets steeper with increasing temperature, indicating that the resistance decreases at elevated temperature. Figure 6b shows the initial resistance R_0, extracted from the VI slope in Figure 6a, as a function of chamber temperature. The R_0 reduces from 15.9 kΩ at 25 °C down to about 10 kΩ at 85 °C with the rate of about −0.1 kΩ/°C. The reduction of resistance with increasing temperature is caused by thermally assisted variable range hopping across the CNT network, which facilitates more charge transport at higher temperature above room temperature.[53,54] The impact of temperature variations when the nanocomposites are stretched is shown in Figure 6a. The reduction rate ($\Delta R/\Delta T$) at 30% strain is almost similar to the unstretched one of about −0.1 kΩ/°C. However, when we stretch the nanocomposites by more than 30%, the impact starts getting more significant approaching as high as −2 kΩ/°C at 90% strain. Mitigation is clearly needed to reduce the temperature effect on the sensing properties, in particular, when the nanocomposites are stretched more than 30%. For instance, one can hybridize CNTs and graphite film to minimize the temperature effect.[53] However, it is beyond the scope of the present study and we leave the issue out for future studies.

CONCLUSIONS

In conclusion, we have succeeded in fabricating a highly elastic and sensitive SWCNT−PEEU nanocomposite yarn using a low hydrothermal process. We have obtained a high GF value of up

https://doi.org/10.1021/acsomega.1c05543
ACS Omega 2021, 6, 34866−34875

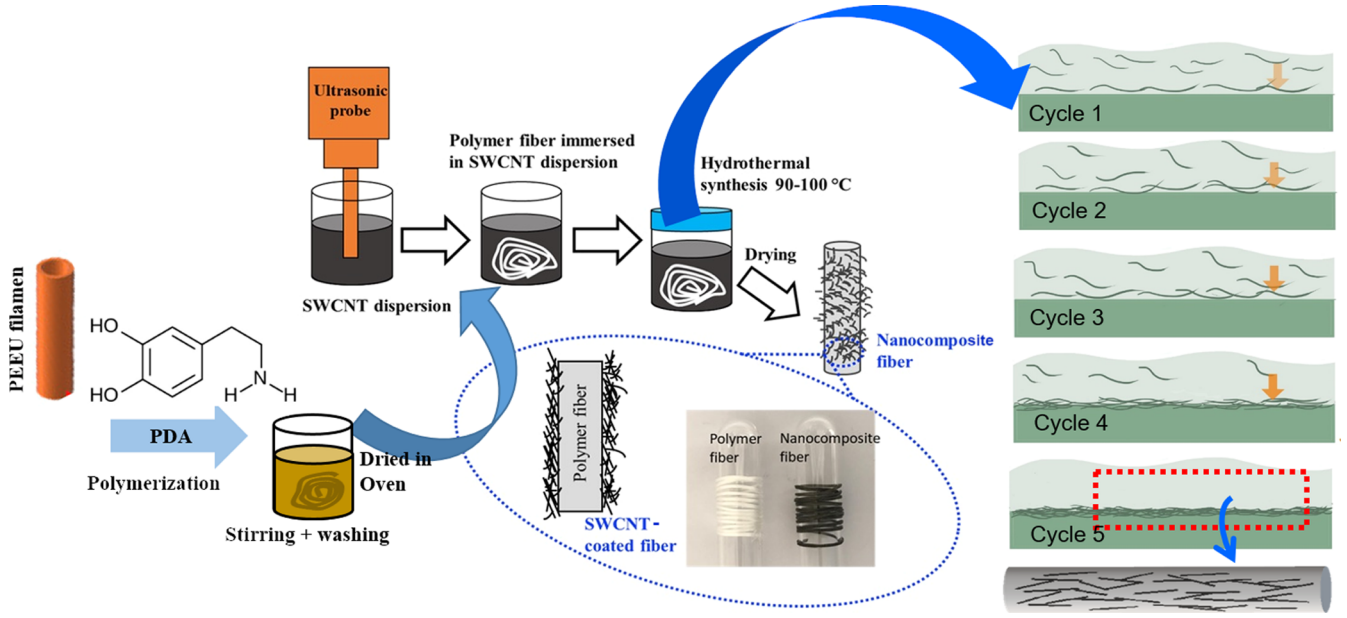

Figure 7. Schematic illustration of hydrothermal fabrication of the SWCNT−PEEU nanocomposite.

to 28.5 at a maximum stretch of 600%. Nanocomposite yarns with a low SWCNT concentration of 1.5% by weight have excellent electrical and sensing properties, capable of detecting a fine human motion and a fast response time.

The SWCNT network and configuration on the PEEU polymer substrate are crucial for determining the transport properties. We find that the piezoresistivity of our nanocomposites is affected by temperature due to a thermally activated hopping mechanism. Future works are needed to minimize the temperature effect, for instance, by hybridizing our nanocomposites with graphite films as demonstrated in ref 53.

EXPERIMENTAL METHODS

Materials. We purchased SWCNTs with purity 95%, 0.1−0.2 nm diameter. and 3−30 μm length from Chengdu Alpha Nano Tech. Co. Ltd. PEEU yarn as the polymer substrate was commercially purchased from a traditional sewing shop. Dopamine hydrochloride, tris(hydroxymethyl)aminomethane, and sodium dodecyl sulfate BioXtra 99% were purchased from Sigma-Aldrich.

Fabrication Methods of the PEEU−SWCNT Nanocomposite. As shown in Figure 7, prior to mixing the yarn with SWCNTs, we washed it with ethanol, acetone, and DI water, respectively. We dissolved (5 mg/mL) dopamine in 50 mL of DI water with the pH adjusted to 8.5 by gently adding 1 M Tris HCl solution (pH 8.8). We then immersed the yarn (50 cm long and 500 μm in diameter) in the dopamine solution under stirring at 60 rpm for 24 h at room temperature. Finally, we washed the yarn thoroughly with DI water and dried it at 60 °C in an oven. In the meantime, we separately prepared a 20 mg SWCNT dispersion using a probe sonication in DI water containing 100 mg of SDS. We then hydrothermally processed the pretreated PEEU yarn in SWCNT solution at 90 °C hydrolysis, for 3 h in each cycle and dried in an oven at 50 °C for 30 min. After drying, we measured it electrical resistance at room temperature. The electrical conductivity improves gradually with repeating the hydrothermal process up to 5 cycles as schematically shown in Figure 7 and demonstrated in Figure 1(f-4).

Structural and Physical Characterization. It is imperative to characterize various physical properties of a bare PEEU yarn and SWCNT−PEEU nanocomposites in the first place. The carbon structure of SWCNTs was evaluated by a modular iHR320 Raman spectrometer (Horiba Scientific, Japan) with a 532 nm excitation laser. The morphological surface of the nanocomposite was observed by a scanning electron microscope, JEOL JSM IT300 at 15 kV, to see the effect of PDA treatment on the interfacial bonding between SWCNTs and the PEEU substrate. Tensile tests were carried out by a universal testing machine Yasuda equipped with a 100 N load cell. The nanocomposite yarn was clamped in 25.4 mm distance and stretched out at the rate of 10 mm/min. The wash durability of the nanocomposite was tested by stirring the samples in water for 2 h at room temperature and 50 °C. The process was repeated three times to evaluate the interfacial bonding strength between SWCNTs and the polymer substrate.

Electrical Transport Properties. We measured a change in the voltage−current (VI) curve due to mechanical deformation using a Keithley 2450 source meter unit. During the mechanical deformation test, the nanocomposite sample was placed in a linear motor stage with both sample ends clamped firmly. We swept the voltage bias from −1 to +1 V and monitored its electrical current each time at a different strain value, ranging from 0 to 600%. The electrical resistance is simply determined from the inverse of the VI slope. We also measured electromechanical properties of the sample placed in a linear motor stage in the control chamber of temperature scan up to 90 °C and humidity.

AUTHOR INFORMATION

Corresponding Authors

Mohammad Hamzah Fauzi − *Research Center for Physics, Indonesian Institute of Sciences, South Tangerang 15314, Indonesia*; Email: mohammad.hamzah.fauzi@lipi.go.id

https://doi.org/10.1021/acsomega.1c05543
ACS Omega 2021, 6, 34866−34875

Rike Yudianti − *Research Center for Physics, Indonesian Institute of Sciences, South Tangerang 15314, Indonesia;* orcid.org/0000-0001-6946-707X; Email: rike.yudianti@lipi.go.id

Authors

Riyani Tri Yulianti − *Research Center for Physics, Indonesian Institute of Sciences, South Tangerang 15314, Indonesia*

Yuyun Irmawati − *Research Center for Physics, Indonesian Institute of Sciences, South Tangerang 15314, Indonesia*

Fredina Destyorini − *Research Center for Physics, Indonesian Institute of Sciences, South Tangerang 15314, Indonesia*

Muhammad Ghozali − *Research Center for Chemistry, Indonesian Institute of Sciences, South Tangerang 15314, Indonesia*

Andi Suhandi − *Research Center for Physics, Indonesian Institute of Sciences, South Tangerang 15314, Indonesia*

Surip Kartolo − *Research Center for Physics, Indonesian Institute of Sciences, South Tangerang 15314, Indonesia*

Andri Hardiansyah − *Research Center for Physics, Indonesian Institute of Sciences, South Tangerang 15314, Indonesia*

Joon-Hyun Byun − *Korea Institute of Materials Science, Changwon 642-831, South Korea;* orcid.org/0000-0003-3528-9206

Complete contact information is available at: https://pubs.acs.org/10.1021/acsomega.1c05543

Notes

The authors declare no competing financial interest.

■ ACKNOWLEDGMENTS

This work was supported by the KIMS, South Korea under KIMS-Asia Countries Project and Research Center for Physics, Indonesian Institute of Sciences for supporting research facilities. We thank Abdulloh Rifai for his technical assistance in setting up the temperature-humidity chamber.

■ REFERENCES

(1) Syduzzaman, Md.; Patwary, S.; Farhana, K. Smart textiles and nano-technology: A general overview. *J. Text. Sci. Eng.* **2015**, *05*, 1−7.

(2) Zaporotskova, I. V.; Boroznina, N. P.; Parkhomenko, Y. N.; Kozhitov, L. V. Carbon nanotubes: Sensor properties. A review. *Mod. Electron. Mater.* **2016**, *2*, 95−105.

(3) Camilli, L.; Passacantando, M. Advances on sensors based on carbon nanotubes. *Chemosensors* **2018**, *6*, 62.

(4) Liu, Y.; Wang, H.; Zha, W.; Zhang, M.; Qin, H.; Xie, Y. Flexible, stretchable sensors for wearable health monitoring: Sensing mechanisms, materials,fabrication strategies and features. *Sensor* **2018**, *18*, 645.

(5) Liu, X.; Zhou, Z.; Wang, T.; Xu, Y.; Lu, K.; Yan, Y. Molecularly imprinted polymers-captivity ZnO nanorods for sensitive and selective detecting environmental pollutant. *Spectrochim. Acta, Part A* **2019**, *228*, 117785.

(6) Xiao, L.; Chen, Z.; Feng, C.; Liu, L.; Bai, Z.-Q.; Wang, Y.; Qian, L.; Zhang, Y.; Li, Q.; Jiang, K.; Fan, S. Flexible, stretchable, transparent carbon nanotube thin film loudspeakers. *Nano Lett.* **2008**, *8*, 4539−4545.

(7) Yudianti, R.; Onggo, H.; Indriyati, S. Role of catalytic synthesis on growth and distribution of platinum nanoparticle on carbon nanotube surface. *Nanosci. Nanotechnol.* **2012**, *2*, 171−177.

(8) Utari, L.; Septiani, N. L. W.; Suyatman, S.; Tapran, N.; Nur, L. O.; Wasisto, H. S.; Yuliarto, B. Wearable carbon monoxide sensors based on hybrid graphene/ZnO nanocomposites. *IEEE Access* **2020**, *8*, 49169−49179.

(9) He, Z.; Byun, J.-H.; Zhou, G.; Park, B.-J.; Kim, T.-H.; Lee, S.-B.; Yi, J.-W.; Um, M.-K.; Chou, T.-W. Effect of MWCNT content on the mechanical and strain-sensing performance of Thermoplastic Polyurethane composite fibers. *Carbon* **2019**, *146*, 701−708.

(10) Lee, H.; Kim, M.-J.; Kim, J.-H.; Lee, J.-Y.; Ji, E.; Capasso, A.; Choi, H.-J.; Shim, W.; Lee, G.-H. Highly flexible graphene nanoplatelet- polydimethylsiloxane strain sensors with proximity-sensing capability Highly fl exible graphene nanoplatelet-polydimethylsiloxane strain sensors with proximity-sensing capability. *Mater. Res. Express* **2020**, *7*, 045603.

(11) Park, H.; Jeong, Y. R.; Yun, J.; Hong, S. Y.; Jin, S.; Lee, S.-J.; Zi, G.; Ha, J. S. Stretchable array of highly sensitive pressure sensors consisting of polyaniline nanofibers and Au-coated polydimethylsiloxane micropillars. *ACS Nano* **2015**, *9*, 9974−9985.

(12) Amjadi, M.; Yoon, Y. J.; Park, I. Ultra-stretchable and skin-mountable strain sensors using carbon nanotubes-Ecoflex nanocomposites. *Nanotechnology* **2015**, *26*, 375501.

(13) Dong, W.; Yao, D.; Yang, L. Soft bimodal sensor array based on conductive hydrogel for driving status monitoring. *Sensors* **2020**, *20*, 1−13.

(14) Zhou, G.; Byun, J.-H.; Oh, Y.; Jung, B.-M.; Cha, H.-J.; Seong, D.-G.; Um, M.-K.; Hyun, S.; Chou, T.-W. Highly sensitive wearable textile-based humidity sensor made of high-strength, single-walled carbon nanotube/poly(vinyl alcohol) filaments. *ACS Appl. Mater. Interfaces* **2017**, *9*, 4788−4797.

(15) Tang, Z.; Jia, S.; Wang, F.; Bian, C.; Chen, Y.; Wang, Y.; Li, B. Highly stretchable core-sheath fibers via wet-spinning for wearable strain sensors. *ACS Appl. Mater. Interfaces* **2018**, *10*, 6624−6635.

(16) Govaert, F.; Vanneste, M. Preparation and application of conductive textile coatings filled with honeycomb structured carbon nanotubes. *J. Nanomater.* **2014**, *2014*, 1−6.

(17) Sadi, M. S.; Pan, J.; Xu, A.; Cheng, D.; Cai, G.; Wang, X. Direct dip-coating of carbon nanotubes onto polydopamine-templated cotton fabrics for wearable applications. *Cellulose* **2019**, *26*, 7569−7579.

(18) Shim, B. S.; Chen, W.; Doty, C.; Xu, C.; Kotov, N. A. Smart electronic yarns and wearable fabrics for human biomonitoring made by carbon nanotube coating with polyelectrolytes. *Nano Lett.* **2008**, *8*, 4151−4157.

(19) Li, L.; Bai, Y.; Li, L.; Wang, S.; Zhang, T. A Superhydrophobic smart coating for flexible and wearable sensing electronics. *Adv. Mater.* **2017**, *29*, 1702517.

(20) Amjadi, M.; Yoon, Y. J.; Park, I. Ultra-stretchable and skin-mountable strain sensors using carbon nanotubes-Ecoflex nanocomposites. *Nanotechnology* **2015**, *26*, 375501.

(21) Dai, H.; Thostenson, E.; Schumacher, T. Processing and Characterization of a Novel Distributed Strain Sensor Using Carbon Nanotube-Based Nonwoven Composites. *Sensors* **2015**, *15*, 17728−17747.

(22) Wood, J. R.; Zhao, Q.; Wagner, H. D. Orientation of carbon nanotubes in polymers and its detection by Raman spectroscopy. *Composites, Part A* **2001**, *32*, 391−399.

(23) Huang, S.; Liang, N.; Hu, Y.; Zhou, X.; Abidi, N. Polydopamine-assisted surface modification for bone biosubstitutes. *BioMed Res. Int.* **2016**, *2016*, 1−9.

(24) Yang, Y.; Qi, P.; Ding, Y.; Maitz, M. F.; Yang, Z.; Tu, Q.; Xiong, K.; Leng, Y.; Huang, N. A biocompatible and functional adhesive amine-rich coating based on dopamine polymerization. *J. Mater. Chem. B* **2015**, *3*, 72−81.

(25) Islam, G. M. N.; Ali, A.; Collie, S. Textile sensors for wearable applications : a comprehensive review Textile sensors for wearable applications : a comprehensive review. *Cellulose* **2020**, *27*, 6103.

(26) Xiao, M.; Zhang, Na.; Zhuang, J.; Sun, Y.; Ren, F.; Zhang, W.; Hou, Z. Degradable poly(ether-ester-urethane)s based on well-defined aliphatic diurethane diisocyanate with excellent shape recovery properties at body temperature for biomedical application. *Polymers* **2019**, *11*, 1−17.

(27) Yan, X.; Itoh, T.; Kitahama, Y.; Suzuki, T.; Sato, H.; Miyake, T.; Ozaki, Y. A Raman spectroscopy study on single-wall carbon

nanotube/polystyrene nanocomposites: mechanical compression transferred from the polymer to single-wall carbon nanotubes. *J. Phys. Chem. C* **2012**, *116*, 17897−17903.
(28) Elashmawi, I. S.; Gaabour, L. H. Raman, morphology and electrical behavior of nanocomposites based on PEO/PVDF with multi-walled carbon nanotubes. *Results Phys.* **2015**, *5*, 105−110.
(29) Dresselhaus, M. S.; Dresselhaus, G.; Saito, R.; Jorio, A. Raman spectroscopy of carbon nanotubes. *Phys. Rep.* **2005**, *409*, 47−99.
(30) Mahajan, A.; Kingon, A.; Kukovecz, Á.; Konya, Z.; Vilarinho, P. M. Studies on the thermal decomposition of multiwall carbon nanotubes under different atmospheres. *Mater. Lett.* **2013**, *90*, 165−168.
(31) Al Sheheri, S. Z.; Al-Amshany, Z. M.; Al Sulami, Q. A.; Tashkandi, N. Y.; Hussein, M. A.; El-Shishtawy, R. M. The preparation of carbon nanofillers and their role on the performance of variable polymer nanocomposites. *Des. Monomers Polym.* **2019**, *22*, 8−53.
(32) Zhang, Q.; Liu, L.; Zhao, D.; Duan, Q.; Ji, J.; Jian, A.; Zhang, W.; Sang, S. Highly sensitive and stretchable strain sensor based on Ag@CNTs. *Nanomaterials* **2017**, *7*, 424.
(33) Muth, J. T.; Vogt, D. M.; Truby, R. L.; Mengüç, Y.; Kolesky, D. B.; Wood, R. J.; Lewis, J. A. Embedded 3D printing of strain sensors within highly stretchable elastomers. *Adv. Mater.* **2014**, *26*, 6307−6312.
(34) Obitayo, W.; Liu, T. A Review: Carbon Nanotube-Based Piezoresistive Strain Sensors. *J. Sens.* **2012**, *2012*, 1−15.
(35) Zhang, H. W.; Wang, J. B.; Ye, H. F.; Wang, L. Parametric variational principle and quadratic programming method for van der Waals force simulation of parallel and cross nanotubes. *Int. J. Solid Struct.* **2007**, *44*, 2783−2801.
(36) He, X. Q.; Kitipornchai, S.; Wang, C. M.; Liew, K. M. Modeling of van der Waals force for infinitesimal deformation of multi-walled carbon nanotubes treated as cylindrical shells. *Int. J. Solid Struct.* **2005**, *42*, 6032−6047.
(37) Li, Z.-Y.; Zhai, W.; Yu, Y.-F.; Li, G. J.; Zhan, P. F.; Xu, J. W.; Zheng, G. Q.; Dai, K.; Liu, C. T.; Shen, C. Y. An ultrasensitive, durable and stretchable strain sensor with crack-wrinkle structure for human motion monitoring. *Chin. J. Polym. Sci.* **2021**, *39*, 316.
(38) Cai, L.; Song, L.; Luan, P.; Zhang, Q.; Zhang, N.; Gao, Q.; Zhao, D.; Zhang, X.; Tu, M.; Yang, F.; Zhou, W.; Fan, Q.; Luo, J.; Zhou, W.; Ajayan, P. M.; Xie, S. Super-stretchable, transparent carbon nanotube-based capacitive strain sensors for human motion detection. *Sci. Rep.* **2013**, *3*, 3048.
(39) Chen, J.; Zhu, Y.; Jiang, W. A stretchable and transparent strain sensor based on sandwich-like PDMS/CNTs/PDMS composite containing an ultrathin conductive CNT layer. *Compos. Sci. Technol.* **2020**, *186*, 107938.
(40) Park, P. W.; Kim, T.; Kim, D.; Hong, Y.; Gong, H. S. Measurement of finger joint angle using stretchable carbon nanotube strain sensor. *PLoS One* **2019**, *14*, No. e0225164.
(41) Shi, J.; Li, X.; Cheng, H.; Liu, Z.; Zhao, L.; Yang, T.; Dai, Z.; Cheng, Z.; Shi, E.; Yang, L.; Zhang, Z.; Cao, A.; Zhu, H.; Fang, Y. Graphene reinforced carbon nanotube networks for wearable strain sensors. *Adv. Funct. Mater.* **2016**, *26*, 2078−2084.
(42) Zhao, S.; Zhang, G.; Gao, Y.; Deng, L.; Li, J.; Sun, R.; Wong, C. P. Strain-driven and ultrasensitive resistive sensor/switch based on conductive alginate/nitrogen-doped carbon-nanotube-supported ag hybrid aerogels with pyramid design. *ACS Appl. Mater. Interfaces* **2014**, *6*, 22823.
(43) Amjadi, M.; Pichitpajongkit, A.; Lee, S.; Ryu, S.; Park, I. Highly stretchable and sensitive strain sensor based on silver nanowire-elastomer nanocomposite. *ACS Nano* **2014**, *8*, 5154−5163.
(44) Yamada, T.; Hayamizu, Y.; Yamamoto, Y.; Yomogida, Y.; Izadi-Najafabadi, A.; Futaba, D. N.; Hata, K. A stretchable carbon nanotube strain sensor for human-motion detection. *Nat. Nanotechnol.* **2011**, *6*, 296−301.
(45) Liang, B.; Zhang, Z.; Chen, W.; Lu, D.; Yang, L.; Yang, R.; Zhu, H.; Tang, Z.; Gui, X. Direct patterning of carbon nanotube via stamp contact printing process for stretchable and sensitive sensing devices. *Nano-Micro Lett.* **2019**, *11*, 92.
(46) Liang, B.; Lin, Z.; Chen, W.; He, Z.; Zhong, J.; Zhu, H.; Tang, Z.; Gui, X. Ultra-stretchable and highly sensitive strain sensor based on gradient structure carbon nanotubes. *Nanoscale* **2018**, *10*, 13599−13606.
(47) Wang, C.; Li, X.; Gao, E.; Jian, M.; Xia, K.; Wang, Q.; Xu, Z.; Ren, T.; Zhang, Y. Carbonized silk fabric for ultrastretchable, highly sensitive, and wearable strain sensors. *Adv. Mater.* **2016**, *28*, 6640−6648.
(48) He, Z.; Zhou, G.; Byun, J.-H.; Lee, S.-K.; Um, M.-K.; Park, B.; Kim, T.; Lee, S. B.; Chou, T.-W. Highly stretchable multi-walled carbon nanotube/thermoplastic polyurethane composite fibers for ultrasensitive, wearable strain sensors. *Nanoscale* **2019**, *11*, 5884−5890.
(49) Tan, C.; Dong, Z.; Li, Y.; Zhao, H.; Huang, X.; Zhou, Z.; Jiang, J.-W.; Long, Y.-Z.; Jiang, P.; Zhang, T.-Y.; Sun, B. A high performance wearable strain sensor with advanced thermal management for motion monitoring. *Nat. Commun.* **2020**, *11*, 3530.
(50) Tadakaluru, S.; Thongsuwan, W.; Singjai, P. Stretchable and flexible high-strain sensors made using carbon nanotubes and graphite films on natural rubber. *Sensors* **2014**, *14*, 868−876.
(51) Qin, Q.; Zhu, Y. Static Friction between Silicon Nanowires and Elastomeric Substrates. *ACS Publ* **2011**, *5*, 7404−7410.
(52) Suhr, J.; Koratkar, N.; Keblinski, P.; Ajayan, P. Viscoelasticity in carbon nanotube composites. *Nat. Mater.* **2005**, *4*, 134−137.
(53) Amjadi, M.; Sitti, M. Self-sensing paper actuators based on graphite−carbon nanotube hybrid films. *Adv. Sci.* **2018**, *5*, 1800239.
(54) Gong, S.; Zhu, Z. H.; Li, Z. Electron tunnelling and hopping effects on the temperature coefficient of resistance of carbon nanotube/polymer nanocomposites. *Phys. Chem. Chem. Phys.* **2017**, *19*, 5113−5120.
(55) Nankali, M.; Nouri, N. M.; Navidbakhsh, M.; Geran Malek, N.; Amindehghan, M. A.; Montazeri Shahtoori, A.; Karimi, M.; Amjadi, M. Highly stretchable and sensitive strain sensors based on carbon nanotube-elastomer nanocomposites: The effect of environmental factors on strain sensing performance. *J. Mater. Chem. C* **2020**, *8*, 6185−6195.

https://doi.org/10.1021/acsomega.1c05543
ACS Omega 2021, 6, 34866−34875